Available online at www.sciencedirect.com
SCIENCE DIRECT®
Journal of Membrane Science 249 (2005) 245–249
journal of MEMBRANE SCIENCE
www.elsevier.com/locate/memsci

Rapid communication

Permeability and selectivity analysis for ultrafiltration membranes

Amit Mehta, Andrew L. Zydney*

Department of Chemical Engineering, The Pennsylvania State University, University Park, PA 16802, USA

Received 22 June 2004; received in revised form 16 September 2004; accepted 24 September 2004
Available online 23 November 2004

Abstract

One of the major challenges facing end-users of ultrafiltration membranes is the difficulty in comparing membrane products provided by different manufacturers and made from different polymeric or ceramic materials. In this short communication, we examine the trade-off between permeability and selectivity for different ultrafiltration membranes using data for bovine serum albumin. Results for a number of different ultrafiltration membranes fall along, or below, an "upper bound" that reflects the current state-of-the-art in commercial ultrafiltration membranes, analogous to the Robeson Plot used to analyze the performance of gas separation membranes. The shape of this upper bound is consistent with a theoretical analysis of solute and solvent transport through a membrane composed of a parallel array of cylindrical pores having a log–normal pore size distribution. These results provide a framework that can be used to analyze the performance of new ultrafiltration membranes, an approach that was demonstrated using data for a prototype negatively charged ultrafiltration membrane.

Keywords: Permeability; Selectivity analysis; Ultrafiltration membranes; Transport; Porous membranes

1. Introduction

Ultrafiltration is currently used for the concentration of a wide range of protein products, including recombinant therapeutics, industrial enzymes, and a variety of food and beverage products [1,2]. Since the development of ultrafiltration as a viable industrial process in the 1960s, there have been literally thousands of different UF membranes sold commercially. For example, the chapter on *Ultrafiltration* in the 1992 Edition of the Membrane Handbook [3] lists 26 different manufacturers of UF membranes, many of which produced several different series of membranes (e.g., polysulfone, cellulose acetate, and regenerated cellulose), with each series containing membranes having a range of pore size or molecular weight cut-off. The most recent edition of Munir Cheryan's Ultrafiltration and Microfiltration Handbook [4] lists more than 90 companies providing membrane and/or module systems for ultrafiltration and microfiltration.

One of the major challenges facing end-users of ultrafiltration membranes is the enormous difficulty in comparing membrane products provided by different manufacturers and made from different polymeric or ceramic materials. Ultrafiltration membranes are normally rated by their nominal molecular weight cut-off, which is typically defined as the molecular weight of a solute that has a rejection coefficient of 90%. However, there is no standardization in this 90% value, and different manufacturers measure the rejection using solutes with very different physical properties and under very different operating conditions. The net result is that two membranes rated as having the same nominal molecular weight cut-off can have very different pore size and performance characteristics. In addition, the molecular weight of a solute with 90% rejection provides no quantitative information on the molecular weight cut-off required to achieve the 99 or 99.9% retention currently targeted for applications of ultrafiltration in the purification of high value proteins [1,5].

In the area of gas separation membranes, Robeson [6] presented a very simple approach for comparing membranes made from different materials and different manufacturers. The separation factor α, which is equal to the ratio of the

* Corresponding author. Tel.: +1 814 863 7113; fax: +1 814 865 7846.
E-mail address: zydney@engr.psu.edu (A.L. Zydney).

0376-7388/$ – see front matter © 2004 Elsevier B.V. All rights reserved.
doi:10.1016/j.memsci.2004.09.040

permeability of the more permeable gas to that of the less permeable species, was plotted as a function of the permeability of the more permeable gas on a log–log scale. Data for a large number of different membranes all clustered below a critical line, or upper bound, which is often referred to in the gas separations community as the "line of death" since there are few (if any) membranes that provide a combination of selectivity and permeability above this limit. The original discussion of the "Robeson Plot" has become one of the most highly cited papers in the gas membrane separations literature with more than 250 citations as of early 2004.

The objectives of this short communication were: (1) to develop an analogous "Robeson Plot" suitable for examining the trade-offs between permeability and selectivity for different ultrafiltration membranes; (2) to examine the theoretical basis for the underlying relationship in this plot; and (3) to use this Robeson Plot to examine the performance characteristics of recently developed charged ultrafiltration membranes.

2. Permeability–selectivity analysis

In its most basic form, ultrafiltration is a pressure-driven process designed to remove solvent (typically water) and small solutes (e.g., salts and sugars) from a large macromolecule. Since mass transport is dominated by convection, the rate of mass transport for both the product and the small impurities is proportional to the filtrate flux and the corresponding solute sieving coefficients (S_i), where S_i is equal to the ratio of the solute concentration in the filtrate to that in the bulk (feed) solution. The sieving coefficient is simply equal to $1 - R$ where R is the protein rejection coefficient. Since the filtration velocity is the same for all species, the separation factor would simply be equal to the ratio of the sieving coefficients for the small impurities to that of the protein product:

$$\alpha = \frac{S_{\text{small}}}{S_{\text{protein}}} \tag{1}$$

Since the small impurities pass freely through the membrane, $S_{\text{small}} \approx 1$ and the separation factor is simply equal to the reciprocal of the protein sieving coefficient.

The permeability of interest in an ultrafiltration process is that with respect to the solvent:

$$L_p = \frac{J_v}{\Delta P} \tag{2}$$

where J_v is the volumetric filtrate flux (volume flow rate per membrane area) and ΔP is the transmembrane pressure driving force. L_p is often referred to as the hydraulic permeability since water is the typical solvent, and the data are often normalized by the solvent viscosity to account for the effects of temperature. The literature includes a wide range of different units for the permeability, with the filtrate flux given in m/s, L/m^2/h (LMH), or gal/ft^2/day (gfd) and the pressure driving force given in Pa, mmHg, psi, or atm (among others).

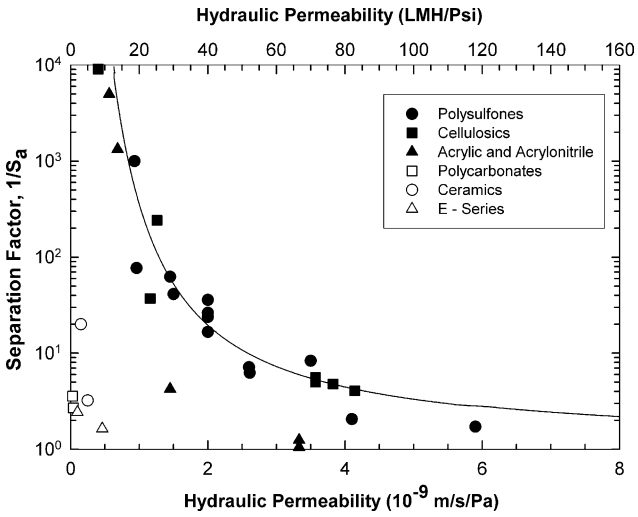

Fig. 1. Selectivity–permeability trade-off for ultrafiltration membranes using BSA as the model protein. Solid curve represents model calculations using a log–normal pore size distribution with $\sigma/\bar{r} = 0.2$ and $\varepsilon/\delta_m = 1\ \mu m^{-1}$.

Fig. 1 shows the selectivity–permeability trade-off using literature data [7–14] for a large number of UF membranes with bovine serum albumin (BSA) as the protein of interest due to the large amount of available data on BSA ultrafiltration. The separation factor has been evaluated using Eq. (1) based on the actual protein sieving coefficient (S_a) to account for differences in concentration polarization within the various modules used in these studies: stirred cells, hollow fibers, screened channel cassettes, and ceramic monoliths. The values thus provide a measure of the intrinsic separation factor or selectivity for the membrane. The actual sieving coefficients were evaluated from experimental data for the observed sieving coefficients ($S_o = C_{\text{filtrate}}/C_{\text{feed}}$) using a stagnant film model [15]:

$$S_a = \frac{S_0}{(1 - S_0)\exp(J_v/k) + S_0} \tag{3}$$

The mass transfer coefficients (k) in the different modules were calculated using the correlations given by Zeman and Zydney [15]. Literature results were taken under conditions where the actual sieving coefficient was approximately equal to asymptotic sieving coefficient, and where to $J_v/k < 10$ to avoid highly polarized conditions. Care was taken to use data obtained during the initial stages of the ultrafiltration where membrane fouling was likely to be low. The data obtained by Opong and Zydney [7] were for membranes that had been pre-adsorbed in the protein solution prior to the ultrafiltration experiment, with the hydraulic permeability evaluated after this initial protein adsorption. Thus, the separation factor and permeability in these studies were both evaluated for membranes in the same physical "state".

The filled circles in Fig. 1 represent data for polysulfone and polyethersulfone membranes, the dominant materials used in ultrafiltration, while the filled squares represent results for cellulosics. Acrylic and acrylonitrile mem-

branes are represented by filled triangles. Results for other materials including ceramics (zirconium) and polycarbonate track-etched membranes are shown with open symbols. These membranes have nominal molecular weight cut-offs (provided by the manufacturers) ranging from 30 to 1000 kDa compared to the 69 kDa molecular weight of BSA. The data for this wide range of membranes all tend to cluster along, and below, a single curve, which represents the upper limit (or upper bound) of current ultrafiltration membranes. All of the existing membranes display a similar trade-off between separation factor and permeability; membranes with high separation factors will have relatively low permeability while those with high permeabilities have low separation factors. The ideal UF membrane would have a very high separation factor (providing very high product retention and yield of the desired protein) and very high permeability (providing the potential for very high filtration rates). Such a membrane would be located in the upper right hand corner of the plot, a region that is currently inaccessible by existing UF membranes.

Although most of the membranes in Fig. 1 cluster along the same curve, there are a small number of outliers that seem to have unusually low separation factors and/or permeabilities. The open squares at a permeability of 0.03 and 0.04×10^{-9} m/s/Pa are for polycarbonate track-etch membranes, which are typically used only for laboratory studies. These membranes have very low porosity (typically around 5%) and a homogenous pore morphology, with an effective thickness of 10 μm compared to the 0.5 μm skin thickness of commercial asymmetric membranes. This combination of low porosity and large thickness gives a very low permeability structure at the same separation factor. The open triangles in Fig. 1 are for E-series membranes produced by Desalination Systems and available in spiral wound modules [13]. It is unclear why these particular membranes, or the ceramic membranes studies by Millesime et al. [14], have such low permeabilities.

3. Theoretical analysis

In order to obtain additional insights into the trade-off between separation factor and permeability, theoretical calculations were performed for an idealized UF membrane consisting of a parallel array of cylindrical pores having a distribution of pore radii. Fluid flow through each pore is described by the Hagen–Poiseuille equation, with the permeability for the membrane as a whole given as [16]:

$$\bar{L}_p = \frac{\varepsilon}{8\mu\delta_m} \frac{\int_0^\infty n(r) r^4 \, dr}{\int_0^\infty n(r) r^2 \, dr} \tag{4}$$

where ε is the membrane porosity; δ_m, the membrane thickness; μ, the solvent viscosity; and $n(r)$, the pore size distribution. The r^4 dependence in the numerator comes from the Hagen–Poiseuille equation, while the r^2 dependence in the denominator is from the cross-sectional area of the cylindrical pores.

The protein sieving coefficient can also be evaluated by integration over the pore size distribution:

$$\bar{S}_a = \frac{\int_0^\infty S_a(r) n(r) r^4 \, dr}{\int_0^\infty n(r) r^4 \, dr} \tag{5}$$

$S_a(r)$, the actual sieving coefficient in a pore with radius r, was evaluated using the expression developed by Zeman and Wales [17]:

$$S_a(r) = (1-\lambda)^2[2-(1-\lambda)^2] \exp(-0.7146\lambda^2) \tag{6}$$

where $\lambda = a/r$ with a being the protein radius. Note that Eq. (6) is only valid if protein transport through the membrane pore is dominated by convection, which is a reasonable approximation for most ultrafiltration systems. Eq. (6) gives values of S_a that are within 2% of more complex expressions over the full range of λ [15].

Theoretical calculations were performed using a log–normal pore size distribution [16]:

$$n(r) = \frac{n_0}{r\sqrt{2\pi}} [\ln(1+(\sigma/\bar{r})^2)]^{-1/2} \times \exp\left\{ -\frac{(\ln(r/\bar{r})[1+(\sigma/\bar{r})^2]^{1/2})^2}{2 \ln[1+(\sigma/\bar{r})^2]} \right\} \tag{7}$$

where $\bar{r}$ is the mean and σ^2 the variance of the distribution, respectively. The log–normal density function has been used extensively in the past to describe membrane pore size distributions [18]. It is particularly convenient for this type of analysis since it is only defined for positive values of the pore radius.

The solid curve in Fig. 1 was developed from Eqs. (4)–(7) with the coefficient of variation kept at a constant value of $\sigma/\bar{r} = 0.2$. For these calculations, the radius of BSA was taken as $a = 36.5 \times 10^{-10}$ m (36.5 Å) and the viscosity of water was taken as 0.001 Pa s. The ratio of the membrane porosity to the membrane thickness was chosen as $\varepsilon/\delta_m = 1\ \mu m^{-1}$, which is consistent with a membrane having a porosity of 0.5 and a skin thickness of 0.5 μm. Calculations were performed by varying the mean pore size (keeping $\sigma/\bar{r}$ and ε/δ_m fixed), with the separation factor and the permeability for each value of $\bar{r}$ plotted as the solid curve in Fig. 1. Membranes with large mean pore radius have high permeability but low separation factors (i.e., poor protein retention), while membranes with small mean pore radius have very high separation factors but low permeability. The model calculations are in surprisingly good agreement with the upper bound for the experimental data, suggesting that the best membranes currently available have pore size distributions that are at least approximately described by a log–normal density function with coefficient of variation equal to about 0.2.

The effects of the membrane properties on the trade-off between the permeability and separation factor is examined

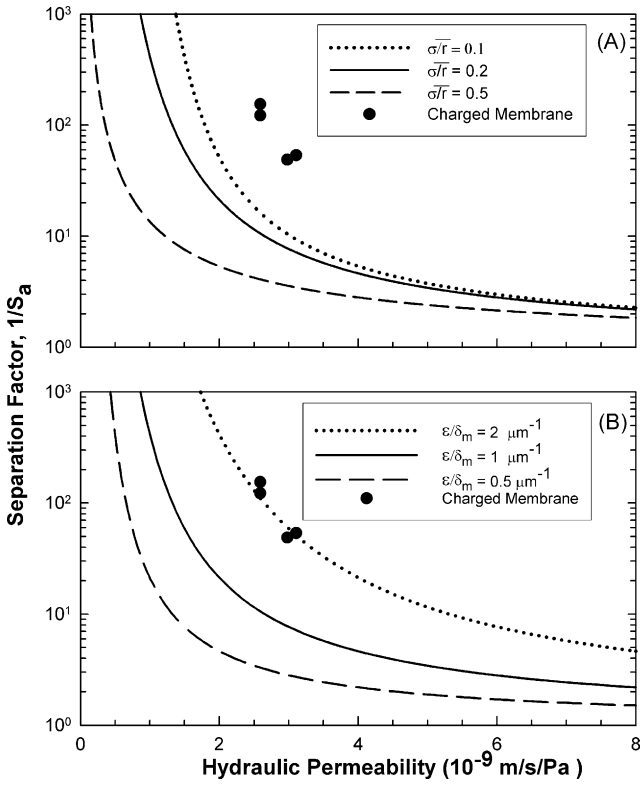

Fig. 2. Influence of membrane properties on trade-off between the separation factor and permeability: (A) effect of breadth of pore size distribution and (B) effect of porosity to thickness ratio. Filled circles represent data for prototype charged CRC membranes.

in more detail in Fig. 2. The upper panel shows simulations with different values of the coefficient of variation (with $\varepsilon/\delta_m = 1\ \mu m^{-1}$), while the lower panel shows results for membranes with different values of ε/δ_m (with $\sigma/\bar{r} = 0.2$). As the coefficient of variation is reduced from 0.5 to 0.1, the upper bound moves up and towards the right since the tighter pore size distribution reduces the number of very large pores that are permeable to the protein of interest. The upper bound also moves up and to the right as ε/δ_m is increased, corresponding to an increase in the membrane porosity and/or a reduction in the skin thickness. The curve with $\varepsilon/\delta_m = 2$ would correspond to a membrane with $\varepsilon = 0.5$ and $\delta_m = 0.25\ \mu m$, which is considerably thinner than existing ultrafiltration membranes. In addition, it is important to note that protein diffusion may become important with such thin membranes, which would cause an increase in protein transmission and thus a reduction in the separation factor relative to that predicted using Eq. (6) [7].

4. Electrically charged UF membranes

The filled circles in Fig. 2 represent data for the ultrafiltration of BSA using prototype negatively charged composite regenerated cellulose (CRC) membranes [19] prepared by surface modification of commercially available CRC membranes provided by Millipore. This involved the covalent attachment of sulfonic acid groups to the base cellulose using a proprietary chemistry [19]. Ultrafiltration experiments were performed at pH 7.4 in a 10 mM phosphate buffer solution, with this low ionic strength chosen to maximize the electrostatic repulsion between the negatively charged BSA and the negatively charged membrane. This electrostatic exclusion causes a dramatic increase in the separation factor, with relatively little change in the membrane permeability. Data obtained with the neutral CRC membrane, or with the negatively charged membrane but at high salt concentrations, gave results that are in good agreement with the upper bound for conventional UF membranes (represented very well by the solid curve in Fig. 2). These data clearly demonstrate that electrically charged ultrafiltration membranes can provide a dramatic improvement in ultrafiltration performance; the permeability at a given separation factor is approximately twice as large as that of a comparable neutral membrane while the separation factor at a given permeability is improved by 15-fold. That level of improvement also appears to be considerably better than what could be obtained by a two-fold reduction in the coefficient of variation, and it is similar to what would be achieved with a two-fold reduction in membrane skin thickness (but without concerns about protein diffusion, mechanical stability, or defects). The performance characteristics of these electrically charged membranes will be the subject of a future manuscript.

5. Discussion

The selectivity–permeability analysis, or “Robeson Plot”, developed in this manuscript provides a very convenient means for comparing the performance characteristics of different ultrafiltration membranes. In this work, literature data for BSA sieving through various UF membranes were analyzed using this simple graphical approach. In addition, a theoretical model was developed based on a membrane composed of a parallel array of cylindrical pores having a log–normal size distribution. The model calculations were in good agreement with the experimental data, demonstrating that the relationship between the selectivity and permeability is a direct result of the hydrodynamic interactions that govern both solute and solvent transport through the membrane pores.

This selectivity–permeability analysis also provides a framework that can be used to analyze the performance of new ultrafiltration membranes. This was demonstrated using data for prototype ultrafiltration membranes developed by attaching a sulfonic acid moiety to existing composite regenerated cellulose membranes. These charge-modified membranes provide a much better combination of separation factor and permeability than existing ultrafiltration membranes due to the strong electrostatic exclusion of the negatively

charged protein from the negatively charged membrane. The performance of these charge-modified membranes also exceeds what would be expected for membranes having a much tighter pore size distribution, suggesting that the addition of electrical charge may be much more effective than attempts to control the membrane pore size.

The data and analysis presented in this manuscript were focused on the behavior of ultrafiltration membranes for protein concentration (or buffer exchange) using BSA. Similar plots could also be constructed for other proteins, allowing one to examine the behavior of membranes with larger or smaller nominal molecular weight cut-offs. In addition, a very similar approach could be used to analyze the behavior of ultrafiltration membranes used for selective protein separations, with the separation factor now given by the ratio of the sieving coefficients for the two proteins of interest [19–21]. This approach could provide an attractive framework for the selection and development of high performance membranes appropriate for protein separations.

Acknowledgements

The authors would like to acknowledge useful discussions with Robert van Reis and Vassia Tegoulia in Bioprocess Development at Genentech Inc.

References

[1] R. van Reis, A.L. Zydney, Protein ultrafiltration, in: M.C. Flickinger, S.W. Drew (Eds.), Fermentation, Biocatalysis, and Bioseparation: Encyclopedia of Bioprocess Technology, John Wiley & Sons Inc., 1999, pp. 2197–2214.
[2] W.K. Wang, Membrane Separations in Biotechnology, second ed., Marcel Dekker Inc., 2001.
[3] S.S. Kulkarni, E.W. Funk, N.N. Li, Membranes, in: W.S.W. Ho, K.K. Sirkar (Eds.), Membrane Handbook, Chapman and Hall, London, 1992.
[4] M. Cheryan, Ultrafiltration and Microfiltration Handbook, Technomic Publishing Co. Inc., Lancaster, 1998.
[5] P. Mulherkar, R. van Reis, Flex test: a fluorescent dextran test for UF membrane characterization, J. Membr. Sci. 236 (2004) 171.
[6] L. Robeson, Correlation of separation factor versus permeability for polymeric membranes, J. Membr. Sci. 62 (1991) 165.
[7] W.S. Opong, A.L. Zydney, Diffusive and convective protein transport through asymmetric membranes, AIChE J. 37 (1991) 1497.
[8] K.D. Miller, S. Weitzel, V.G.J. Rodgers, Reduction of membrane fouling in the presence of high polarization resistance, J. Membr. Sci. 76 (1992) 77.
[9] S. Nakatsuka, A.S. Michaels, Transport and separation of proteins by ultrafiltration through sorptive and non-sorptive membranes, J. Membr. Sci. 69 (1992) 189.
[10] R. Shukla, M. Balakrishnan, G.P. Agarwal, Bovine serum albumin–hemoglobin fractionation: significance of ultrafiltration system and feed solution characteristic, Bioseparation 9 (2000) 7.
[11] N.S. Pujar, A.L. Zydney, Electrostatic and electrokinetic interactions during protein transport through narrow pore membranes, Ind. Eng. Chem. Res. 33 (1994) 2473.
[12] A.G. Fane, C.J.D. Fell, A.G. Waters, Ultrafiltration of protein solutions through partially permeable membranes—the effect of adsorption and solution environment, J. Membr. Sci. 16 (1983) 211.
[13] P. Pradanos, A. Hernandez, Cross-flow ultrafiltration through asymmetric polysulfonic membranes. I. Retention curves and pore size distributions, Biotechnol. Bioeng. 47 (1995) 617.
[14] L. Millesime, J. Dulieu, B. Chaufer, Fractionation of proteins with modified membranes, Bioseparation 6 (1996) 135.
[15] L.J. Zeman, A.L. Zydney, Microfiltration and Ultrafiltration: Principles and Applications, Marcel Dekker Inc., 1996.
[16] S. Mochizuki, A.L. Zydney, Theoretical analysis of pore size distribution effects on membrane transport, J. Membr. Sci. 82 (1993) 211.
[17] L.J. Zeman, M. Wales, Polymer solute rejection by ultrafiltration membranes, in: A.F. Turbak (Ed.), Membranes, vol. II, Hyperfiltration and Ultrafiltration Uses, ACS Symposium Series No. 54, American Chemical Society, Washington, DC, 1981.
[18] A.L. Zydney, P. Aimar, M. Meireles, J.M. Pimbley, G. Belfort, Use of the log–normal probability density function to analyze membrane pore size distributions: Functional forms and discrepancies, J. Membr. Sci. 91 (1994) 293.
[19] R. van Reis, Charged filtration membranes and uses therefor, World Patent WO 01/08792 A2 (2001).
[20] R. van Reis, Tangential flow filtration process and apparatus, US Patent 5,256,294 (1993).
[21] R. van Reis, J.M. Brake, J. Charkoudian, D.B. Burns, A.L. Zydney, High performance tangential flow filtration using charged membranes, J. Membr. Sci. 159 (1999) 133.